University of Reading

Shrub height and crown projection area are effective predictors in aboveground biomass models for multi-stemmed European hazel

Article

Published Version

Creative Commons: Attribution 4.0 (CC-BY)

Open Access

Pajtík, J., Konôpka, B., Barka, I., Merganicova, K. and Lukac, M. ORCID: https://orcid.org/0000-0002-8535-6334 (2025) Shrub height and crown projection area are effective predictors in aboveground biomass models for multi-stemmed European hazel. Forest Ecosystems, 13. 100316. ISSN 2197-5620 doi: 10.1016/j.fecs.2025.100316 Available at https://centaur.reading.ac.uk/122055/

It is advisable to refer to the publisher's version if you intend to cite from the work. See Guidance on citing.

To link to this article DOI: http://dx.doi.org/10.1016/j.fecs.2025.100316

Publisher: Elsevier

All outputs in CentAUR are protected by Intellectual Property Rights law, including copyright law. Copyright and IPR is retained by the creators or other copyright holders. Terms and conditions for use of this material are defined in the End User Agreement.

University of Reading

www.reading.ac.uk/centaur

CentAUR

Central Archive at the University of Reading

Reading's research outputs online

Forest Ecosystems 13 (2025) 100316

Contents lists available at ScienceDirect

Forest Ecosystems

journal homepage: www.keaipublishing.com/cn/journals/forest-ecosystems

Shrub height and crown projection area are effective predictors in aboveground biomass models for multi-stemmed European hazel

Jozef Pajtík [a], Bohdan Konôpka [a,b], Ivan Barka [a], Katarína Merganičová [b,c], Martin Lukac [b,d,*]

[a] National Forest Centre – Forest Research Institute Zvolen, T. G. Masaryka 2175/22, SK, 960 01, Zvolen, Slovak Republic
[b] Czech University of Life Sciences Prague, Faculty of Forestry and Wood Sciences, Kamýcká 129, Prague 6, CZ – 165 21, Suchdol, Czech Republic
[c] Slovak Academy of Sciences, Institute of Landscape Ecology, SK, 949 01, Nitra, Slovak Republic
[d] School of Agriculture, Policy and Development, University of Reading, RG6 6AR, UK

ARTICLE INFO

Keywords:
Aboveground biomass model
Biomass partitioning
Shrub upper height
Canopy projection area
Leaf area index

ABSTRACT

While numerous allometric models exist for estimating biomass in trees with single stems, models for multi-stemmed species are scarce. This study presents models for predicting aboveground biomass (AGB) in European hazel (*Corylus avellana* L.), growing in multi-stemmed shrub form. We measured the size and harvested the biomass of 30 European hazel shrubs, drying and weighing their woody parts and leaves separately. AGB (dry mass) and leaf area models were established using a range of predictors, such as the upper height of the shrub, number of shoots per shrub, canopy projection area, stem base diameter of the thickest stem, and the sum of cross-sectional areas of all stems at the stem base. The latter was the best predictor of AGB, but the most practically useful variables, defined as relatively easy to measure by terrestrial or aerial approaches, were the upper height of the shrub and the canopy projection area. The leaf biomass to AGB ratio decreased with the shrub's height. Specific leaf area of shaded leaves increases with shrub height, but that of leaves at the top of the canopy does not change significantly. Given that the upper shrub height and crown projection of European hazel can be estimated using remote sensing approaches, especially UAV and LIDAR, these two variables appear the most promising for effective measurement of AGB in hazel.

1. Introduction

European hazel (*Corylus avellana* L.) is a deciduous shrub with a woody growth habit, typically reaching a maximum height of around 10 m. As a pioneer species, its broad distribution extends across Europe, from southern Scandinavia to the Mediterranean regions, where its maximum lifespan stretches to about 90 years (De Rigo et al., 2016). Colonising open spaces or growing as an understory species, hazel often establishes itself following disturbance or the cessation of grazing. Highly adaptive, hazel readily colonises abandoned agricultural lands and is commonly found in hedges, thickets, and small woodlands. The propagation of hazel occurs both generatively, through nuts, and vegetatively, via stem sprouts or root suckers. Its ubiquity across the European landscape and its rapid growth have led to numerous traditional applications. These range from hazelnut consumption (Solar and Stampar, 2011) to the use of stems in construction and crafts (Allegrini et al., 2022), as well as harnessing its woody biomass for bioenergy (Zambon et al., 2016).

Due to its inherently low stature and tendency to form multi-stem shrubs, European hazel has traditionally garnered little interest from the wood processing industry. As a result, it is often deemed undesirable in conventional forestry practices focused on optimising timber yield. Consequently, European hazel is routinely removed during early thinning operations to favour species with perceived higher commercial value (Thysell, 2000). Its exclusion from standard forestry yield tables exacerbates the scarcity of documentation regarding its contribution to forest stand biomass. Similarly, in agricultural landscapes where European hazel is relatively common, comprehensive insights into its productivity, biomass, or ecological role are lacking. In a rare investigation, Šebeň (2018) estimated that approximately 15% of woody growing stock on non-forest land in Europe could be attributed to 'other softwood broadleaves', a category in which hazel likely plays a significant role. Given the current emphasis on sustainable forestry and the expansion of agroforestry in Europe (Mosquera-Losada et al., 2023), it is plausible that European hazel will increasingly contribute to fulfilling objectives such

* Corresponding author. Slovak Academy of Sciences, Institute of Landscape Ecology, SK, 949 01, Nitra, Slovak Republic.
E-mail address: m.lukac@reading.ac.uk (M. Lukac).

Peer review under the responsibility of Editorial Office of Forest Ecosystems.

https://doi.org/10.1016/j.fecs.2025.100316
Received 10 September 2024; Received in revised form 11 February 2025; Accepted 12 February 2025
2197-5620/© 2025 The Authors. Publishing services by Elsevier B.V. on behalf of KeAi Communications Co. Ltd. This is an open access article under the CC BY license (http://creativecommons.org/licenses/by/4.0/).

as afforestation, carbon sequestration, or biodiversity enhancement (Terasaki Hart et al., 2023).

European hazel is highly suitable for delivering multiple benefits within forestry and agricultural landscapes. The leaf litter from this species exhibits superior biochemical properties and palatability to livestock compared to most other broadleaved tree species (De Rigo et al., 2016). Hazel foliage, typical for its high concentration of base cations, enhances the buffering capacity of acidic soils (Marschner and Noble, 2000) and augments nutrient availability in forest soil (Mohr and Topp, 2005). When growing in mono-specific stands, hazel shrubs create distinctive habitats that foster flora and fauna biodiversity (Tiunov and Scheu, 1999). As a pioneer species, hazel is typical for a dynamic canopy development (Finsinger et al., 2006), with rapid changes in resource allocation to maximize light interception. Such changes within and across years are critical for competition and habitat creation (Niinemets et al., 1998). The species' notable ability to coppice and resprout makes it an excellent candidate for short-rotation coppice, particularly in countries where non-native species are discouraged. Its productivity allows for its utilisation in biofuels, biogas, or biochar manufacture, thereby positioning European hazel as a versatile species within the circular economy framework (Allegrini et al., 2022).

Given the considerable potential of European hazel, there is a pressing need to establish a reliable aboveground biomass (AGB) model. Such a model is crucial for estimating hazel's contribution to woody biomass in a given area, assessing its yield potential, or improving the accuracy of greenhouse gas flux reporting in the land use sector (Grassi et al., 2022). Allometric relationships, widely employed for biomass estimation in single-stem trees (Konôpka et al., 2011; Le Goff and Ottorini, 2022; Petersson et al., 2012; Xiang et al., 2021), utilise mathematical functions to convert easily measurable tree characteristics into biomass. Stem diameter is often the most precise and readily measurable characteristic (West and West, 2009). However, parameterising allometric models becomes more challenging in woody plants with multiple stems. Although allometric models have been previously developed for coppiced species such as *Eucalyptus globulus* (Zewdie et al., 2009), *Robinia pseudoacacia* L. (Carl et al., 2017), *Salix* spp. (Mosseler et al., 2014), or *Populus* spp. (Oliveira et al., 2017), they all rely on measuring stem diameter and the number of stems, which is laborious and resource-demanding.

Allometric models predicting tree biomass are widely developed and used. This paper aims to construct models for estimating AGB in coppiced or multi-stem European hazel shrubs and test their accuracy. In addition, we sought to describe the development of hazel foliage as a function of shrub height, as it is the key driver of biomass production. Our investigation involves testing the effectiveness of a range of predictor variables to optimise the trade-off between ease of measurement and the accuracy of biomass predictions. We describe the properties of hazel foliage as it forms the canopy and drives growth. Lastly, we discuss predictor variable usefulness against the likely application of close-range remote sensing techniques.

2. Material and methods

2.1. Site and tree measurements

The fieldwork for this study was conducted during the second half of the 2022 growing season in three mountain ranges: Strážovské vrchy, Štiavnické vrchy, and Nízke Tatry, representing the conditions of the Inner Western Carpathians, Slovakia, Europe (see Fig. 1). Sampled sites are located on land classified as forest and in the following Forest Administration Units: Rajecké Teplice, Šášov, and Predajná. Due to the land designation as forest, the occurrence of European hazel is reported at the level of forest administration units, which guided our selection of possible locations. All sites were situated on mesotrophic cambisols and ranged from 470 to 910 m above sea level. The local forester then indicated relevant plots where forest harvesting occurred within the last 15 years. Ten shrubs, at least 50 m apart (approximately ten times the estimated height) and composed of pure hazel, were randomly selected at each location. Each shrub consisted of several tens of relatively uniform stems, avoiding shrubs with a single dominant stem surrounded by secondary stem sprouts (see Fig. 2).

The crown projection area of each shrub was established by measuring its radius in four perpendicular directions using a rolling measuring tape with a precision of ±1.0 cm (Table 1). We then determined the maximum height of the shrub using a measuring stick with a precision of ±1.0 cm. Subsequently, all stems of the shrub were cut at ground level. We counted the number of stems in the individual shrub and measured their diameters at the stem base to establish the sum of their cross-sectional areas.

All stems in each shrub were then cut down at ground level. We randomly collected fifteen leaves from each shrub, five each from the

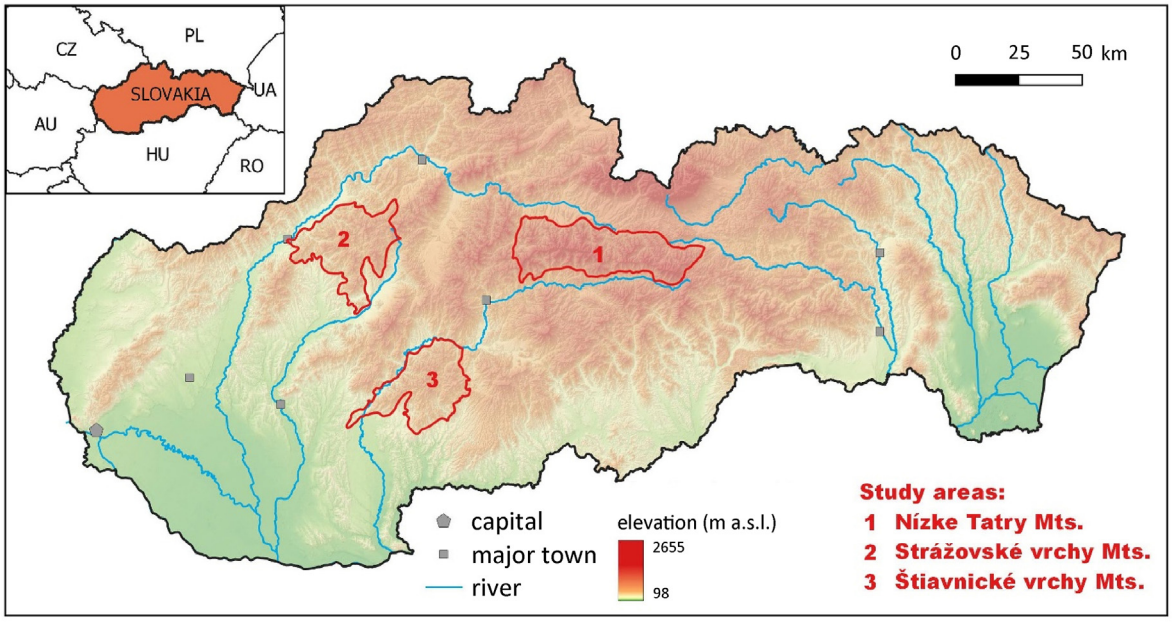

Fig. 1. Location of the study areas for research of aboveground European hazel biomass, Inner Western Carpathians, Slovakia.

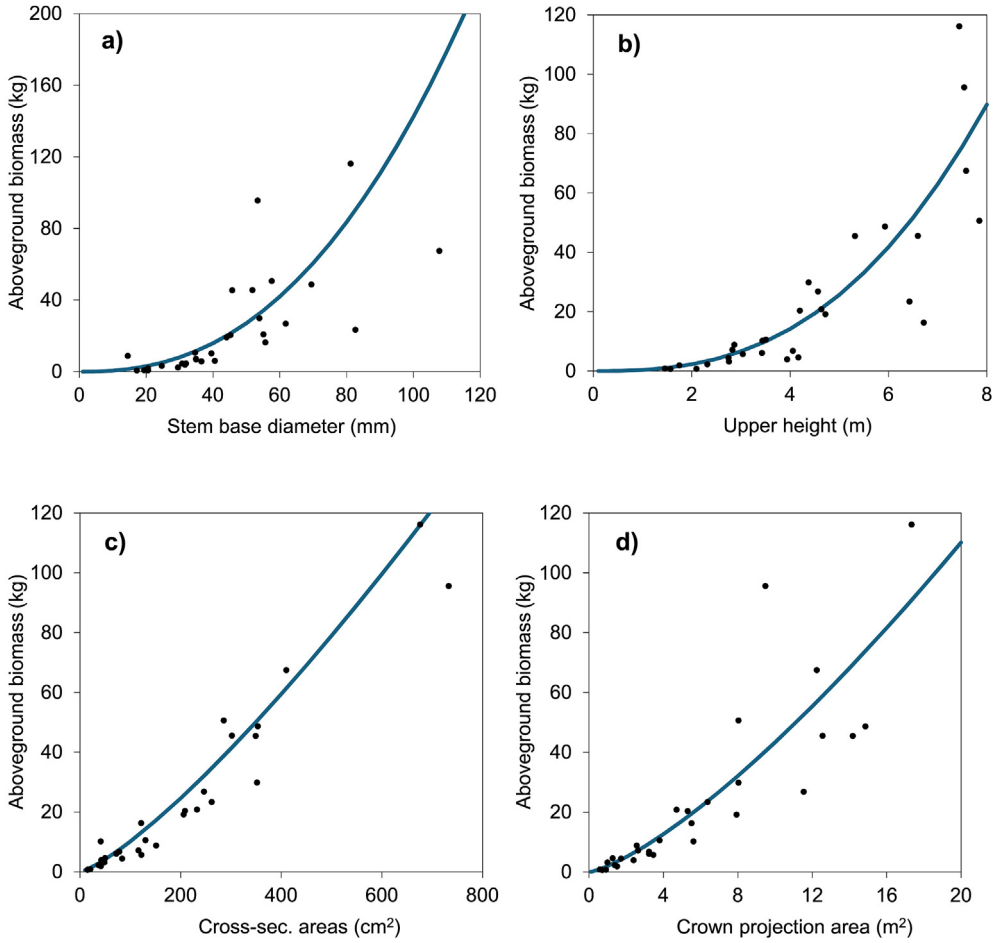

Fig. 2. Model fits predicting aboveground biomass (lines) as a function of the stem base diameter of the thickest stem (**a**), maximum height (**b**), the sum of cross-sectional areas of all stems at base (**c**), and crown projection area (**d**) of a single European hazel shrub. Dots represent measured values in 30 individual shrubs.

Table 1
Key variables describing the European hazel shrubs, as measured in this study: d_0 – stem base diameter of the thickest stem, h – upper height of the shrub, N – number of stems per shrub, CPA – shrub crown projection area, S_g – sum of cross-sectional areas of all stems in the shrub, B_{wb} – wood under bark biomass per shrub, B_l – leaf biomass per shrub, B_{ab} – aboveground biomass per shrub (wood under bark + foliage), w_f – weight of the leaf, LA – leaf area, SLA – specific leaf area. The same below.

Parameter	Mean	S.D.	Min	Max	25th percentile	75th percentile	Skewness
d_0 (mm)	44.27	21.41	14.50	107.80	30.80	55.15	1.07
h (m)	4.33	1.92	1.46	7.85	2.83	5.93	0.42
N	20.63	10.26	6.00	51.00	13.00	26.00	1.03
CPA (m^2)	5.81	4.79	0.59	17.35	1.73	8.04	0.91
S_g (cm^2)	193.73	182.48	15.17	733.10	48.97	285.92	1.53
B_{wb} (kg)	23.44	28.71	0.64	116.13	4.42	29.83	1.88
B_l (kg)	2.18	2.15	0.11	7.43	0.44	3.95	1.14
B_{ab} (kg)	25.63	30.74	0.79	123.56	4.91	33.78	1.82
w_f (g)	0.25	0.13	0.04	0.68	0.15	0.31	1.01
LA (cm^2)	49.18	16.01	17.93	122.97	38.34	58.95	0.83
SLA (cm^2·g^{-1})	234.89	91.99	65.94	508.15	160.12	305.63	0.38

crown's upper, middle, and lower parts. The leaves were scanned within one or two days while fresh (Epson Expression 10000 XL), placed in labelled paper bags and dried at 95 °C for 24 h. Leaf scans were analysed using Easy Leaf Area software (https://github.com/heaslon/Easy-Leaf-Area) following the Easlon and Bloom protocol (Easlon and Bloom, 2014). After drying, the leaves were weighed with a precision of ±0.0001 g (Precisa 40SM-200A). After leaf sub-sampling, whole stems with branches and bulk foliage were cut into sections, placed in labelled paper bags and transported to the laboratory. Bulk foliage was manually separated from the woody parts, and both components were stored in a well-ventilated room for a few days. All biomass samples were dried in a large-capacity oven at 105 °C for 4–5 days until constant weight. Dried samples were weighed using a digital laboratory scale with a precision of ±0.01 g (Radwag, WLT 3/6/X).

2.2. Calculations and modelling

The construction of models focused on estimating the dry mass of foliage, woody parts and total AGB of individual hazel shrubs where these can be identified. We also developed models for closed-canopy hazel stands by predicting the same variables per 1 m^2 of the area covered by this shrub. We tested the performance of the following

predictors: diameter at stem base of the thickest stem d_0, height of the thickest stem ("top height") h, number of stems in the shrub N, shrub crown projection CPA, and the sum of cross-sectional areas at the base of all stems in the shrub S_g. All predictors were derived from field measurements. We used power-form allometric functions:

$$W_i = b_0 X_1^{b_1} X_2^{b_2} \ldots X_n^{b_n} \quad (1)$$

which were log-transformed to remove the effect of heteroscedasticity and then reverse-transformed to the following form:

$$W_i = \mathrm{e}^{(b_0 + b_1 \ln(X_1) + b_2 \ln(X_2) \ \ldots \ b_n \ln(X_n))} \lambda \quad (2)$$

where

W_i – the amount of biomass in the i^{th} shrub part (kg of dry mass of a shrub shrub); X_1, X_2, …, X_n – predictors; b_0, b_1, …, b_n – equation coefficients, λ – logarithmic transformation bias.

Statistical descriptors of the performance of models with a single independent variable are provided in Table 2. Based on the knowledge that the dry weight of individual fractions is least influenced by the number of stems and the base diameter of the dominant stem, we did not consider these variables in further model formation with multiple independent variables. Statistical characteristics of models with multiple independent variables are provided in Table 3.

When calculating the dry weight of fractions per 1 m^2 of canopy area, the biomass stock of individual fractions $W_i m$ was the dependent variable, with the height of the dominant stem h and the leaf area index LAI selected as independent variables. We selected these predictors as close-range remote sensing technology makes them relatively easy to establish. In our study, LAI is a variable derived from the weight of W and leaf area LA of 15 leaves collected from each shrub across the canopy depth. Descriptive statistics of these sampled leaves are provided in Table 1. Based on these measured values, we derived the specific leaf area SLA at the leaf level according to the equation:

$$\mathrm{SLA} = \mathrm{LA} \times W^{-1} \quad (3)$$

The specific leaf area at the shrub level $\mathrm{SLA}_{\mathrm{shrub}}$ was calculated as the arithmetic mean of SLA values from 15 sampled leaves per shrub. Based on this derived SLA and the dry weight of leaf biomass W_f obtained by drying and weighing all leaves collected from each shrub, we calculated the leaf area $\mathrm{LA}_{\mathrm{shrub}}$ of all leaves at the shrub level:

$$\mathrm{LA}_{\mathrm{shrub}} = \mathrm{SLA}_{\mathrm{shrub}} \times W_f \quad (4)$$

LAI for each shrub was derived based on $\mathrm{LA}_{\mathrm{shrub}}$ and the total area of the crown projection of the shrub CPA:

$$\mathrm{LAI} = \mathrm{LA}_{\mathrm{shrub}} \times \mathrm{CPA}^{-1} \quad (5)$$

The stock of the i-th fraction per 1 m^2 of canopy area was expressed using a logarithmically transformed allometric function similar to the calculations of fraction dry weight at the shrub level:

$$W_i m = \mathrm{e}^{(b_0 + b_1 \ln(X_1) + b_2 \ln(X_2) \ \ldots \ b_n \ln(X_n))} \lambda \quad (6)$$

Model parameters and model performance is detailed in Table 4.

In hazel stands with known canopy cover, it is then possible to derive the stock of biomass components according to:

$$W_i = S \times C \times \mathrm{W}_i m \quad (7)$$

where W_i – dry biomass of i-th component in a stand, S – stand area (m^2), C – canopy cover (from 0 to 1), $W_i m$ – biomass of i-th component per 1 m^2.

K-fold cross-validation of each model was conducted in R programming language v. 4.3.0 to validate the model performance (R Core Team, 2023) using Metrics, Caret and hydroGOF packages. K was set to 5 and 6, with 100 repetitions for each K. The following model performance indicators were calculated as mean values from all runs: mean absolute error (MAE), mean squared error (MSE), absolute root mean square prediction error (RMSPE) and relative root mean square prediction error (RMSPE %).

3. Results

The base diameter of the stems in the sampled European hazel shrubs varied between 14.50 and 107.80 mm, while their heights ranged from 1.46 to 7.85 m (Table 1). The total number of stems per shrub varied between 6 and 51, and the crown projection area ranged from 0.59 to 17.35 m^2. Predictor variables were used to construct biomass models in two steps: individual predictors and their combinations. Among the single predictor models, upper height, mean diameter at stem base, sum of cross-sectional areas on stem bases, and crown projection area of a hazel bush were all effective predictors.

In contrast, the number of stems in a shrub was less suitable (Table 2). The closest relationship was between biomass and the sum of cross-sectional areas at the stem base. In the next step, we combined the best-performing single predictors into the following pairs: shrub height × crown projection area; shrub height × sum of cross-sectional areas; crown projection area × sum of cross-sectional areas; shrub height × crown projection area × sum of cross-sectional areas. The combined models effectively predicted woody, foliage, and total biomass (Table 3). Finally, a model combining all predictors measured in this study resulted in the closest relationship (R^2 was 0.982 for woody parts, 0.973 for foliage, and 0.983 for AGB).

Table 2
Coefficients and model performance of single predictor variable biomass models for European hazel. Predictor variables used to construct the models are: d_0, h, N, CPA, S_g. b_0, b_1 are regression coefficients, S.E. is standard error, P is the p-value of the fit, R^2 is the coefficient of determination, MSE is the mean square error, λ is the logarithmic transformation bias and S.D. is its standard deviation. The same below.

Variables	Component	B_0 (S.E.), P	b_1 (S.E.), P	R^2	MSE	λ	S.D.
d_0	Wood and bark	−6.674 (1.023), <0.001	2.442 (0.276), <0.001	0.743	0.515	1.388	1.808
	Foliage	−7.161 (0.950), <0.001	1.990 (0.257), <0.001	0.690	0.444	1.313	1.479
	Aboveground	−6.380 (0.119), <0.001	2.393 (0.272), <0.001	0.741	0.500	1.375	1.762
H	Wood and bark	−1.368 (0.314), <0.001	2.727 (0.222), <0.001	0.849	0.303	1.132	0.519
	Foliage	−2.696 (0.364), <0.001	2.117 (0.257), <0.001	0.715	0.408	1.183	0.656
	Aboveground	−1.165 (0.317), 0.001	2.662 (0.224), <0.001	0.840	0.310	1.135	0.526
N	Wood and bark	−2.379 (1.330), 0.085	1.624 (0.457), 0.001	0.319	1.366	1.988	2.692
	Foliage	−4.248 (1.060), <0.001	1.528 (0.364), <0.001	0.395	0.868	1.548	1.636
	Aboveground	−2.214 (1.300), 0.100	1.607 (0.447), 0.001	0.324	1.306	1.931	2.552
CPA	Wood and bark	0.455 (0.126), 0.001	1.369 (0.077), <0.001	0.922	0.157	1.077	0.434
	Foliage	−1.411 (0.104), <0.001	1.160 (0.063), <0.001	0.926	0.106	1.050	0.334
	Aboveground	0.602 (0.121), <0.001	1.346 (0.074), <0.001	0.925	0.145	1.070	0.410
S_g	Wood and bark	−3.838 (0.341), <0.001	1.294 (0.070), <0.001	0.926	0.149	1.088	0.591
	Foliage	−5.051 (0.279), <0.001	1.097 (0.058), <0.001	0.931	0.099	1.060	0.483
	Aboveground	−3.620 (0.327), <0.001	1.273 (0.068), <0.001	0.929	0.136	1.081	0.568

Table 3
Biomass models for European hazel constructed by combinations of the following predictor variables: h, N, CPA, S_g. In the model, b_0, b_1, b_2, b_3, are regression coefficients. W: wood, B: bark, F: foliage, ABVG: aboveground.

Variables	Component	b_0 (S.E.), P	b_1 (S.E.), P	b_2 (S.E.), P	b_3 (S.E.), P	R^2	MSE	λ	S.D.
h, CPA	W + B	−0.350 (0.229), 0.138	1.035 (0.263), <0.001	0.934 (0.127), <0.001		0.951	0.102	1.046	0.314
	F	−1.459 (0.237), <0.001	0.062 (0.273), 0.883	1.134 (0.132), <0.001		0.926	0.110	1.050	0.333
	ABVG	−0.126 (0.227), 0.582	0.937 (0.261), 0.001	0.952 (0.126), <0.001		0.950	0.101	1.045	0.311
h, S_g	W + B	−3.307 (0.243), <0.001	1.132 (0.191), <0.001	0.861 (0.087), <0.001		0.969	0.065	1.037	0.361
	F	−4.914 (0.297), <0.001	0.292 (0.232), 0.220	0.986 (0.105), <0.001		0.935	0.097	1.055	0.444
	ABVG	−3.129 (0.244), <0.001	1.046 (0.191), <0.001	0.873 (0.087), <0.001		0.967	0.066	1.037	0.363
CPA, S_g	W + B	−1.926 (0.412), <0.001	0.700 (0.124), <0.001	0.692 (0.117), <0.001		0.967	0.070	1.033	0.279
	F	−3.437 (0.323), <0001	0.591 (0.097) <0.001	0.589 (0.092), <0.001		0.971	0.043	1.019	0.202
	ABVG	−1.742 (0.389), <0.001	0.688 (0.115), <0.001	0.681 (0.109), <0.001		0.970	0.060	1.028	0.254
h, CPA, S_g	W + B	−2.203 (0.311), <0.001	0.783 (0.165), <0.001	0.464 (0.107), <0.001	0.596 (0.089), <0.001	0.982	0.038	1.017	0.198
	F	−3.367 (0.327), <0.001	−0.198 (0.174), 0.266	0.651 (0.110), <0.001	0.614 (0.094), <0.001	0.973	0.042	1.018	0.193
	ABVG	−1.984 (0.302), <0.001	0.684 (0.161), <0.001	0.481 (0.102), <0.001	0.597 (0.087), <0.001	0.983	0.036	1.016	0.191

Table 4
Models predicting biomass per unit area for European hazel on the basis of h and LAI.

Variables	Component (kg·m^{-2})	b_0 (S.E.), P	b_1 (S.E.), P	b_2 (S.E.), P	R^2	MSE	λ	S.D.
h	Wood and bark	−0.278 (0.180), 0.134	0.916 (0.127), <0.001		0.659	0.099	1.047	0.320
	Foliage	−1.606 (0.189), <0.001	0.305 (0.134), 0.030		0.162	0.110	1.051	0.334
	Aboveground	−0.075 (0.178), 0.678	0.850 (0.126), <0.001		0.630	0.097	1.046	0.315
LAI	Wood and bark	−0.733 (0.294), 0.019	0.882 (0.150), <0.001		0.561	0.128	1.064	0.400
	Foliage	−2.525 (0.141), <0.001	0.697 (0.072), <0.001		0.776	0.030	1.014	0.175
	Aboveground	−0.578 (0.268), 0.040	0.862 (0.137), <0.001		0.594	0.107	1.053	0.363
h, LAI	Wood and bark	−1.045 (0.181), <0.001	0.674 (0.096), <0.001	0.572 (0.100), <0.001	0.849	0.046	1.021	0.211
	Foliage	−2.531 (0.148), <0.001	0.014 (0.078), 0.860	0.691 (0.082), <0.001	0.776	0.031	1.014	0.175
	Aboveground	−0.858 (0.172), <0.001	0.604 (0.091), <0.001	0.850 (0.126), <0.001	0.849	0.041	1.019	0.201

The carbon density of vegetation is a parameter useful for monitoring and reporting carbon storage in ecosystems. Standard forest mensuration relies on the number of stems per hectare and their size as the fundamental variables driving carbon density, which is not practical for multi-stemmed species such as hazel. We, therefore, combined the height and the LAI of each shrub, two variables that can be estimated with good accuracy by close-range remote sensing, to develop a separate model predicting hazel biomass per unit ground area (Table 4). The results show that woody biomass rapidly increases with height, whereas the related increase in leaf biomass is small (Fig. 3a). As a result, the contribution of leaves to AGB decreases with shrub height, from approximately 15% for a 2-m high hazel shrub to 7% for a shrub 8 m in height.

The dry weight of top, mid and bottom-canopy leaves varied greatly between 0.04 and 0.68 g, while the leaf area showed a much smaller range between 17.93 and 122.97 cm^2 (Table 1). As a result, a large variability of SLA was observed, from 65.94 to 508.15 cm^2·g^{-1}. A very strong effect of canopy position was detected ($p < 0.0001$), with the leaves at the top of the canopy having the smallest (166 ± 71 s.d.) and the most shaded leaves at the bottom of the canopy having the largest mean SLA (293 ± 77 s.d.). The SLA of leaves in the middle and at the top of the canopy increases with shrub height across the range of heights observed in this study ($p = 0.0003$ and 0.0006, respectively), however SLA of leaves at the top of the canopy remains largely unchanged ($p = 0.3304$, Fig. 4a). When compared to other tree species commonly co-occurring with hazel, we see that the SLA of hazel and sycamore increases with shrub height, but that of aspen, birch and hornbeam decreases (Fig. 4b).

We also developed predictive models for leaf area (m^2) and LAI (m^2·m^{-2}) at the shrub level. Leaf area can be modelled fairly accurately based on the projected crown area or the sum of cross-sectional areas at the stem base using one or a combination of these two predictors (Table 4). Interestingly, the maximum measured value of leaf area for a single hazel shrub was 135 m^2 (Fig. 4). Models predicting LAI were less

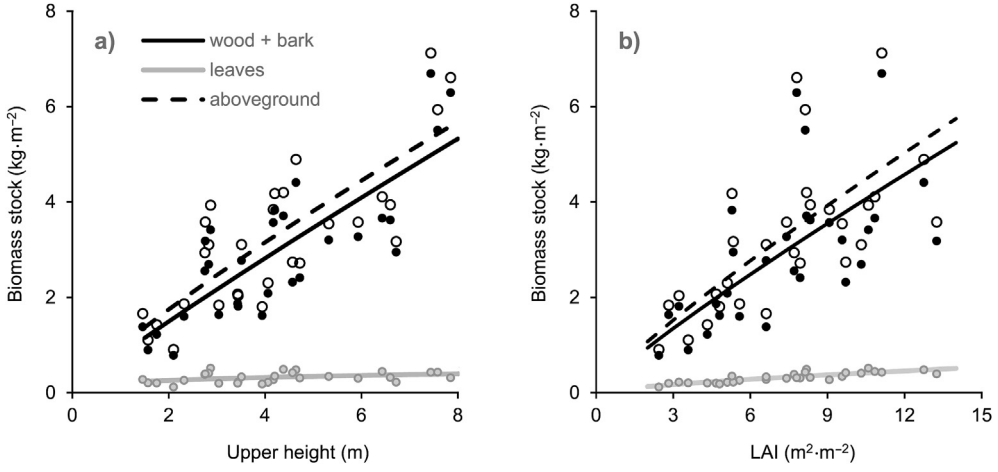

Fig. 3. The relationship between aboveground biomass stock per unit area and its components in European hazel, and shrub height (**a**) and leaf area index (**b**). Dots represent measured values, while lines indicate linear model fits.

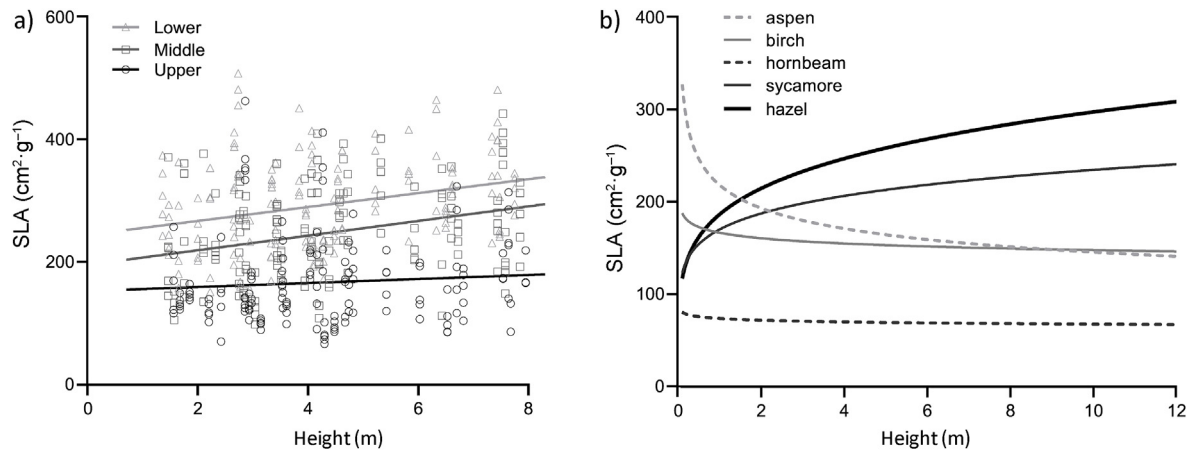

Fig. 4. Specific Leaf Area (SLA) and linear models of hazel foliage at the top, middle and bottom of the canopy dependent on shrub height **(a)**. A comparison of mean SLA in hazel and four other co-occurring deciduous tree species **(b)**, data for aspen, birch, hornbeam and sycamore are from (Konôpka et al., 2021).

accurate, only models combining the crown projection area and the sum of cross-sectional stem areas resulted in a moderately accurate relationship ($R^2_{adj} = 0.546$), with a maximum modelled LAI of nearly 12 $m^2 \cdot m^{-2}$. Finally, a moderate relationship ($R^2 = 0.480$) was found between AGB and LAI (Table 5), indicating that canopy volume rather than light capture capacity of hazel shrubs is a better predictor of biomass and hence carbon content of individual shrubs.

The cross-validation suggested that the accuracy of models increases with an increasing number of independent variables (Table 5). With one independent variable, the models' relative root mean square prediction error (RMSPE) for calculating biomass components ranged between 27% and 74%. With two independent variables, the RMSPE ranged between 20% and 35%, and with three independent variables, it ranged between 19% and 21%.

4. Discussion

4.1. Biomass accumulation and carbon storage

Our observations indicate that hazel foliage is highly responsive to light availability, which is influenced by canopy development and subsequent shading. As a fast-growing pioneer species, hazel adapts its foliage to maximize light and carbon capture per unit of foliage mass. The SLA of hazel leaves is conservative at the top of the canopy, but increases in shaded leaves as the shrub grows larger (Fig. 4a). Shaded leaves become thinner as the plant maximizes leaf area per unit of biomass invested in leaf growth, eventually leading to the shedding of inner canopy leaves. Once the shrub reaches a critical size, hazel retains foliage primarily in the outer "shell" of the crown, with few leaves remaining inside the canopy. Consequently, the LAI remains largely unchanged, while AGB gradually accumulates in the stems beneath the foliage. Additionally, LAI observations are strongly affected by seasonality, as hazel is a deciduous species, requiring remote sensing data collection at specific times. Estimating LAI from remotely sensed datasets is relatively straightforward and accurate (Lee et al., 2023), it can be used as a single predictor or in combination with variables like stand height (Kumar et al., 2015). Our results (Table 4) suggest that using LAI alone as an input in AGB models does not provide satisfactory biomass predictions for European hazel. In combination with height, however, LAI can predict AGB with $R^2 = 0.85$.

Biomass models are important for estimating the fixed and transient carbon pools in forests (e.g., Menéndez-Miguélez et al., 2022; Pajtík et al., 2008) or other ecosystems (e.g., Pasalodos-Tato et al., 2015; Yang et al., 2017). Our models for European hazel show that the tallest hazel shrubs measured in this study, reaching nearly 8 m in height, contain approximately 55 $t \cdot ha^{-1}$ of dry AGB per m^2, of which 8% is annually produced foliage. Seasonal growth rings are not easily recognisable in this species, but based on forest management plans they were between 12 and 14 years old. Our previous research in naturally regenerated forests in the same regions shows that a 13-year-old stand of European beech contains 37 $t \cdot ha^{-1}$ of AGB, with 8% allocated to leaves (Konôpka et al., 2013). Alternatively, a 12-year-old sessile oak forest contains 24 $t \cdot ha^{-1}$ of AGB per m^2, where leaves represent 7% (Pajtík et al., 2011). Hazel is a pioneer species, whereas beech and oak are late-successional, explaining the larger biomass accumulated by hazel during the first decade of growth.

There are two reasons for developing hazel models: its potential for

Table 5
Performance measures in *k*-fold cross-validation of the regression models for biomass of aboveground parts and leaf traits in European hazel. MAE is mean absolute error, MSE is mean squared error, RMSPE is absolute root mean square prediction error, RMSPE % is relative root mean square prediction error. Hazel cluster level and square unit of cluster (m^2) were considered (see asterisk and circle markers in Table). Other abbreviations are explained in the caption of Table 1.

Dependant variable	Predictor	MAE	MSE	RMSPE	RMSPE %
Wood with bark[a]	*h*	11.29	334.25	16.66	72.15
	CPA	11.22	295.19	15.57	66.37
	S_g	13.37	1268.04	19.14	74.13
	h, CPA	7.64	150.42	11.35	48.38
	h, S_g	4.06	67.47	6.85	27.36
	h, CPA, S_g	2.59	15.89	3.61	15.65
Leaves[a]	*h*	1.12	2.53	1.51	72.77
	CPA	0.81	1.32	1.03	47.17
	S_g	1.07	5.81	1.41	61.58
	h, CPA	0.63	1.01	0.90	42.07
	h, S_g	0.48	0.50	0.64	29.27
	h, CPA, S_g	0.38	0.40	0.56	24.88
Aboveground[a] (i.e. wood with bark plus leaves)	*h*	12.33	387.25	17.98	71.50
	CPA	11.87	325.43	16.22	62.93
	S_g	13.56	1101.94	18.72	67.91
	h, CPA	8.09	170.23	12.09	47.43
	h, S_g	4.38	72.71	7.20	26.48
	h, CPA, S_g	2.44	13.59	3.35	13.40
Wood with bark[b]	*h*	0.80	0.85	0.90	31.07
Leaves[b]	*h*	0.09	0.01	0.10	31.01
Aboveground[b]	*h*	0.87	0.99	0.98	30.26

Explanatory notes.
[a] models addressed for hazel cluster level.
[b] models based on m^2 of hazel cluster.

forming a second layer in tall forests and its expansion into former agricultural land. Established forestry practice typically eliminates hazel as a species with little contribution to the economic value of managed forests. However, our comparison shows that more accurate carbon accounting methods or focused applications of green finance may alter this perception. Additionally, many regions in Europe are currently undergoing land use change, where marginal agricultural land is abandoned and reverts to woody vegetation (Csikós and Tóth, 2023). Hazel is one of the species rapidly colonising these areas, highlighting the need for a dependable methodology to estimate its biomass and carbon uptake.

4.2. Predictor variables

Established literature (e.g., Fatemi et al., 2011; Muukkonen, 2007; Tullus et al., 2009) indicates that stem diameter is the most accurate predictor of AGB and its main components (leaves, branches, and stem) in single-stemmed trees. Stem height is generally less correlated with biomass than diameter (Pajtík et al., 2008), but its combination with diameter can marginally improve model performance (Dutcă et al., 2018; Lambert et al., 2005). Several studies have tested the addition of additional tree characteristics, such as age (Wirth et al., 2004) or crown dimensions (Cienciala et al., 2008; Menéndez-Miguélez et al., 2022), in a quest for more accurate AGB prediction. Estimating the biomass of woody species with a shrub-like and multi-stem growth form cannot rely on the same variables or their combination, as establishing their size is simply not practical or even possible. Several attempts to identify predictors and establish allometric relations of AGB in shrub species are documented. Early on, Uso et al. (1997) utilised the volume of the shrub in 10 Mediterranean species, assuming a cylindrical shape. Oyonarte and Cerrillo (2003) developed allometric relations for AGB of 31 shrub species using maximum height, the largest crown diameter, and the smallest crown diameter as predictors. Cerrilo and Oyonarte (2006) tested height, the largest and the smallest crown diameters, and the crown diameter at the bottom of the crown as predictors. Recently, Yao et al. (2021) estimated AGB of six shrub species in Inner Mongolia using crown volume and considering different crown shapes (combinations of maximum and minimum crown diameters in the upper and lower part of the crown). These variables showed some promise, however, their practical implementation at scale is challenging and limits their wider use (Pasalodos-Tato et al., 2015). AGB models for European hazel based on predictors with a reasonable balance between ease of measurement and accuracy are therefore necessary.

4.3. Application of aboveground biomass models

Models estimating the amount of AGB of woody vegetation can have various practical uses, e.g. estimates of productivity and economic output, prediction of biomass accumulation for bioenergy, quantification of carbon sequestration and climate change mitigation potential, optimisation of land use at landscape level and more. To cover the widest range of uses, we created two types of models in this study, predicting AGB in individual hazel shrubs and on an area basis in hazel stands.

The AGB models for individual hazel shrubs are useful for predicting hazel biomass where shrubs are separated from each other, and establishing the size of each shrub is not too difficult. Crown area or shrub height can be measured manually or, increasingly so, with the help of close-range remote sensing technology (Mokroš et al., 2021). Examples of systems where individual shrub models can be applied are agroforestry plantations or newly colonised former agricultural land (Thapa et al., 2023).

An AGB model predicting biomass or carbon content per unit area is more appropriate in hazel stands with closed canopy. Stand height is the most useful prediction variable, eliminating the need to identify individual shrubs as hazel crown overlap. Based on our data, the unit area AGB model using only stand height is more accurate (RMSPE 30%) than the individual shrub AGB model using both height and crown projection area as predictors (RMSPE 47%, Table 5). It is important to point out that we did not validate our unit area model with data from closed-canopy stands; this is a need for future research. In hazel stands with incomplete canopy, correcting the unit area model prediction by canopy closure ratio may be advisable to correctly determine their AGB (Yang et al., 2022). This ratio can presently be determined from the canopy height raster (Likó et al., 2022; Polyakova et al., 2023) and automated determination of species composition in mixed stands (Likó et al., 2022; Polyakova et al., 2023).

Due to the relatively small dimensions of growing hazel shrubs, close-range remotely sensed datasets are necessary (Mokroš et al., 2021; Zhao et al., 2021). Visible spectrum data may be sufficient for the identification of species and for estimating crown cover. However, canopy height measurements require Light Detection and Ranging (LiDAR) or Synthetic Aperture Radar (SAR) interferometric data (Ghosh et al., 2020; Sačkov et al., 2019). The fusion of several types of data from passive and active sensors to determine the height of the vegetation cover has already been demonstrated (Lee and Lee, 2018), but its application is primarily focused on forests (Anderson et al., 2008; Pourshamsi et al., 2021) or open landscapes in dry or polar regions (Bartsch et al., 2020; Hellesen and Matikainen, 2013).

5. Conclusions

We developed well-performing biomass models for European hazel using data from three regions. The sum of cross-sectional areas of hazel shrubs was the most precise predictor; however, we found that the upper height of the shrub and the crown projection area are just as good predictors but far easier to measure. Our models can be combined with remotely sensed observations to automatically estimate hazel biomass or carbon content in individual shrubs and hazel stands. The models can be applied to predict hazel biomass at various scales, ranging from local to national, providing additional data to improve the accuracy of carbon estimates in mixed forests or areas with tree vegetation and on previously agricultural lands with hazel contribution.

CRediT authorship contribution statement

Jozef Pajtík: Writing – review & editing, Writing – original draft, Visualization, Methodology, Investigation, Formal analysis, Data curation, Conceptualization. **Bohdan Konôpka:** Writing – review & editing, Writing – original draft, Project administration, Funding acquisition. **Ivan Barka:** Writing – review & editing, Writing – original draft, Formal analysis, Data curation. **Katarína Merganičová:** Writing – review & editing, Writing – original draft, Conceptualization. **Martin Lukac:** Writing – review & editing, Writing – original draft, Methodology, Investigation, Formal analysis.

Declaration of competing interest

The authors do not declare any conflict of interest.

Funding and Acknowledgements

This research was funded by grants EVA4.0 No. Z.02.1.01/0.0/0.0/16_019/0000803 and ITMS2014 + 313011W580s provided by EU OP RDE in CZ and SK. We acknowledge projects APVV-18-0086, APVV-19-0387, APVV-20-0168, APVV-20-0215 and APVV-22-0056 from the Slovak Research and Development Agency. We also received support from the European Research Executive Agency for ReForest, Grant Agreement Nr: 101060635. The views and opinions expressed are however those of the author(s) only and do not necessarily reflect those of the European Union or the European Research Executive Agency (REA). Neither the European Union nor the granting authority can be held responsible for them.

Appendix A. Supplementary data

Supplementary data to this article can be found online at https://doi.org/10.1016/j.fecs.2025.100316.

References

Allegrini, A., Salvaneschi, P., Schirone, B., Cianfaglione, K., Di Michele, A., 2022. Multipurpose plant species and circular economy: *Corylus avellana* L. as a study case. Front. Biosci.-Landmark 27 (1), 11. https://doi.org/10.31083/j.fbl2701011.

Anderson, J.E., Plourde, L.C., Martin, M.E., Braswell, B.H., Smith, M.-L., Dubayah, R.O., Hofton, M.A., Blair, J.B., 2008. Integrating waveform lidar with hyperspectral imagery for inventory of a northern temperate forest. Remote Sens. Environ. 112 (4), 1856–1870. https://doi.org/10.1016/j.rse.2007.09.009.

Bartsch, A., Widhalm, B., Leibman, M., Ermokhina, K., Kumpula, T., Skarin, A., Wilcox, E.J., Jones, B.M., Frost, G.V., Höfler, A., 2020. Feasibility of tundra vegetation height retrieval from Sentinel-1 and Sentinel-2 data. Remote Sens. Environ. 237, 111515. https://doi.org/10.1016/j.rse.2019.111515.

Carl, C., Biber, P., Landgraf, D., Buras, A., Pretzsch, H., 2017. Allometric models to predict aboveground woody biomass of black locust (*Robinia pseudoacacia* L.) in short rotation coppice in previous mining and agricultural areas in Germany. Forests 8 (9), 328. https://doi.org/10.3390/f8090328.

Cerrillo, R.M.N., Oyonarte, P.B., 2006. Estimation of above-ground biomass in shrubland ecosystems of southern Spain. For. Syst. 15 (2), 197–207. https://doi.org/10.5424/srf/2006152-00964.

Cienciala, E., Apltauer, J., Exnerová, Z., Tatarinov, F., 2008. Biomass functions applicable to oak trees grown in Central-European forestry. J. For. Sci. 54 (3), 109–120. https://doi.org/10.17221/2906-JFS.

Csikós, N., Tóth, G., 2023. Concepts of agricultural marginal lands and their utilisation: a review. Agric. Syst. 204, 103560. https://doi.org/10.1016/j.agsy.2022.103560.

De Rigo, D., Caudullo, G., Houston Durrant, T., San-Miguel-Ayanz, J., 2016. The European Atlas of Forest Tree Species: modelling, data and information on forest tree species. European Atlas of Forest Tree Species. https://doi.org/10.2760/233115.

Dutcă, I., Mather, R., Blujdea, V.N., Ioraș, F., Olari, M., Abrudan, I.V., 2018. Site-effects on biomass allometric models for early growth plantations of Norway spruce (*Picea abies* (L.) Karst.). Biomass Bioenergy 116, 8–17. https://doi.org/10.1016/j.biombioe.2018.05.013.

Easlon, H.M., Bloom, A.J., 2014. Easy leaf area: automated digital image analysis for rapid and accurate measurement of leaf area. Appl. Plant Sci. 2 (7), 1400033. https://doi.org/10.3732/apps.1400033.

Fatemi, F.R., Yanai, R.D., Hamburg, S.P., Vadeboncoeur, M.A., Arthur, M.A., Briggs, R.D., Levine, C.R., 2011. Allometric equations for young northern hardwoods: the importance of age-specific equations for estimating aboveground biomass. Can. J. For. Res. 41 (4), 881–891. https://doi.org/10.1139/x10-248.

Finsinger, W., Tinner, W., van der Knaap, W.O., Ammann, B., 2006. The expansion of *Corylus avellana* in the southern Alps: a key for understanding its early Holocene history in Europe? Quat. Sci. Rev. 25 (5–6), 612–631.

Ghosh, S., Behera, M., Paramanik, S., 2020. Canopy height estimation using sentinel series images through machine learning models in a mangrove forest. Remote Sens 12 (9), 15–19. https://doi.org/10.3390/rs12091519.

Grassi, G., Conchedda, G., Federici, S., Abad Viñas, R., Korosuo, A., Melo, J., Rossi, S., Sandker, M., Somogyi, Z., Tubiello, F.N., 2022. Carbon fluxes from land 2000–2020: bringing clarity on countries' reporting. Earth Syst. Sci. Data Discuss. 1–49. https://doi.org/10.5194/essd-14-4643-2022.

Hellesen, T., Matikainen, L., 2013. An object-based approach for mapping shrub and tree cover on grassland habitats by use of LiDAR and CIR orthoimages. Remote Sens. 5 (2), 558–583. https://doi.org/10.3390/rs5020558.

Konôpka, B., Pajtík, J., Noguchi, K., Lukac, M., 2013. Replacing Norway spruce with European beech: a comparison of biomass and net primary production patterns in young stands. For. Ecol. Manag. 302, 185–192. https://doi.org/10.1016/j.foreco.2013.03.026.

Konôpka, B., Pajtík, J., Šebeň, V., Lukac, M., 2011. Belowground biomass functions and expansion factors in high elevation Norway spruce. Forestry 84 (1), 41–48. https://doi.org/10.1093/forestry/cpq042.

Konôpka, B., Pajtík, J., Šebeň, V., Surový, P., Merganičová, K., 2021. Woody and foliage biomass, foliage traits and growth efficiency in young trees of four broadleaved tree species in a temperate forest. Plants 10 (10), 2155.

Kumar, L., Sinha, P., Taylor, S., Alqurashi, A.F., 2015. Review of the use of remote sensing for biomass estimation to support renewable energy generation. J. Appl. Remote Sens. 9 (1), 097696. https://doi.org/10.1117/1.JRS.9.097696.

Lambert, M.-C., Ung, C., Raulier, F., 2005. Canadian national tree aboveground biomass equations. Can. J. For. Res. 35, 1996–2018. https://doi.org/10.1139/x05-112.

Le Goff, N., Ottorini, J.-M., 2022. Biomass distribution, allocation and growth efficiency in European beech trees of different ages in pure even-aged stands in northeast France. Cent. Eur. For. J. 68, 117–138. https://doi.org/10.2478/forj-2022-0008.

Lee, L.X., Whitby, T.G., Munger, J.W., Stonebrook, S.J., Friedl, M.A., 2023. Remote sensing of seasonal variation of LAI and fAPAR in a deciduous broadleaf forest. Agric. For. Meteorol. 333, 109389. https://doi.org/10.1016/j.agrformet.2023.109389.

Lee, W.-J., Lee, C.-W., 2018. Forest canopy height estimation using multiplatform remote sensing dataset. J. Sensors, 1593129. https://doi.org/10.1155/2018/1593129.

Likó, S.B., Bekő, L., Burai, P., Holb, I.J., Szabó, S., 2022. Tree species composition mapping with dimension reduction and post-classification using very high-resolution hyperspectral imaging. Sci. Rep. 12, 20919. https://doi.org/10.1038/s41598-022-25404-x.

Marschner, B., Noble, A.D., 2000. Chemical and biological processes leading to the neutralisation of acidity in soil incubated with litter materials. Soil Biol. Biochem. 32, 805–813. https://doi.org/10.1016/S0038-0717(99)00209-6.

Menéndez-Miguélez, M., Calama, R., Del Río, M., Madrigal, G., López-Senespleda, E., Pardos, M., Ruiz-Peinado, R., 2022. Species-specific and generalized biomass models for estimating carbon stocks of young reforestations. Biomass Bioenergy 161, 106453. https://doi.org/10.1016/j.biombioe.2022.106453.

Mohr, D., Topp, W., 2005. Hazel improves soil quality of sloping oak stands in a German low mountain range. Ann. For. Sci. 62, 23–29. https://doi.org/10.1051/forest:2004090.

Mokroš, M., Mikita, T., Singh, A., Tomaštík, J., Chudá, J., Wężyk, P., Kuželka, K., Surový, P., Klimánek, M., Zięba-Kulawik, K., 2021. Novel low-cost mobile mapping systems for forest inventories as terrestrial laser scanning alternatives. Int. J. Appl. Earth Obs. Geoinf. 104, 102512. https://doi.org/10.1016/j.jag.2021.102512.

Mosquera-Losada, M.R., Santos, M.G.S., Gonçalves, B., Ferreiro-Domínguez, N., Castro, M., Rigueiro-Rodríguez, A., González-Hernández, M.P., Fernández-Lorenzo, J.L., Romero-Franco, R., Aldrey-Vázquez, J.A., 2023. Policy challenges for agroforestry implementation in Europe. Front. For. Glob. Change 6, 1127601. https://doi.org/10.3389/ffgc.2023.1127601.

Mosseler, A., Major, J., Labrecque, M., Larocque, G., 2014. Allometric relationships in coppice biomass production for two North American willows (*Salix* spp.) across three different sites. For. Ecol. Manag. 320, 190–196. https://doi.org/10.1016/j.foreco.2014.02.027.

Muukkonen, P., 2007. Generalized allometric volume and biomass equations for some tree species in Europe. Eur. J. For. Res. 126, 157–166. https://doi.org/10.1007/s10342-007-0168-4.

Niinemets, Ü., Kull, O., Tenhunen, J.D., 1998. An analysis of light effects on foliar morphology, physiology, and light interception in temperate deciduous woody species of contrasting shade tolerance. Tree Physiol. 18, 681–696.

Oliveira, N., Rodríguez-Soalleiro, R., Hernández, M.J., Cañellas, I., Sixto, H., Pérez-Cruzado, C., 2017. Improving biomass estimation in a Populus short rotation coppice plantation. For. Ecol. Manag. 391, 194–206. https://doi.org/10.1016/j.foreco.2017.02.020.

Oyonarte, P.B., Cerrillo, R.N., 2003. Aboveground phytomass models for major species in shrub ecosystems of western Andalusia. For. Syst. 12, 47–55. https://doi.org/10.5424/1078.

Pajtík, J., Konôpka, B., Lukac, M., 2008. Biomass functions and expansion factors in young Norway spruce (*Picea abies* [L.] Karst) trees. For. Ecol. Manag. 256, 1096–1103. https://doi.org/10.1016/j.foreco.2008.06.013.

Pajtík, J., Konôpka, B., Lukac, M., 2011. Individual biomass factors for beech, oak and pine in Slovakia: a comparative study in young naturally regenerated stands. Trees (Berl.) 25, 277–288. https://doi.org/10.1007/s00468-010-0504-z.

Pasalodos-Tato, M., Ruiz-Peinado, R., Del Río, M., Montero, G., 2015. Shrub biomass accumulation and growth rate models to quantify carbon stocks and fluxes for the Mediterranean region. Eur. J. For. Res. 134, 537–553. https://doi.org/10.1007/s10342-015-0870-6.

Petersson, H., Holm, S., Ståhl, G., Alger, D., Fridman, J., Lehtonen, A., Lundström, A., Mäkipää, R., 2012. Individual tree biomass equations or biomass expansion factors for assessment of carbon stock changes in living biomass–A comparative study. For. Ecol. Manag. 270, 78–84. https://doi.org/10.1016/j.foreco.2012.01.004.

Polyakova, A., Mukharamova, S., Yermolaev, O., Shaykhutdinova, G., 2023. Automated recognition of tree species composition of forest communities using Sentinel-2 satellite data. Remote Sens. 15, 329. https://doi.org/10.3390/rs15020329.

Pourshamsi, M., Xia, J., Yokoya, N., Garcia, M., Lavalle, M., Pottier, E., Balzter, H., 2021. Tropical forest canopy height estimation from combined polarimetric SAR and LiDAR using machine-learning. ISPRS J. Photogramm. Remote Sens. 172, 79–94. https://doi.org/10.1016/j.isprsjprs.2020.11.008.

R Core Team, 2023. R: A Language and Environment for Statistical Computing. R Foundation for Statistical Computing, Vienna.

Sačkov, I., Kulla, L., Bucha, T., 2019. A comparison of two tree detection methods for estimation of forest stand and ecological variables from airborne LiDAR data in central European forests. Remote Sens. 11, 1431. https://doi.org/10.3390/rs11121431.

Šebeň, V., 2018. Národná inventarizácia a monitoring lesov Slovenskej republiky 2015–2016. Lesnícke štúdie 65. Národné lesnícke centrum, Zvolen.

Solar, A., Stampar, F., 2011. Characterisation of selected hazelnut cultivars: phenology, growing and yielding capacity, market quality and nutraceutical value. J. Sci. Food Agric. 91, 1205–1212. https://doi.org/10.1002/jsfa.4300.

Terasaki Hart, D.E., Yeo, S., Almaraz, M., Beillouin, D., Cardinael, R., Garcia, E., Kay, S., Lovell, S.T., Rosenstock, T.S., Sprenkle-Hyppolite, S., 2023. Priority science can accelerate agroforestry as a natural climate solution. Nat. Clim. Change 13, 1179–1190. https://doi.org/10.1038/s41558-023-01810-5.

Thapa, B., Lovell, S., Wilson, J., 2023. Remote sensing and machine learning applications for aboveground biomass estimation in agroforestry systems: a review. Agrofor. Syst. 97, 1097–1111. https://doi.org/10.1007/s10457-023-00850-2.

Thysell, D.R., 2000. Effects of Forest Management on Understory and Overstory Vegetation: a Retrospective Study. U.S. Department of Agriculture, Forest Service, Pacific Northwest Research Station. https://doi.org/10.2737/PNW-GTR-488.

Tiunov, A.V., Scheu, S., 1999. Microbial respiration, biomass, biovolume and nutrient status in burrow walls of *Lumbricus terrestris* L. (I). Soil Biol. Biochem. 31, 2039–2048. https://doi.org/10.1016/S0038-0717(99)00127-3.

Tullus, A., Tullus, H., Soo, T., Pärn, L., 2009. Above-ground biomass characteristics of young hybrid aspen (*Populus tremula* L. × *P. tremuloides* Michx.) plantations on former agricultural land in Estonia. Biomass Bioenergy 33, 1617–1625. https://doi.org/10.1016/j.biombioe.2009.08.001.

Uso, J., Mateu, J., Karjalainen, T., Salvador, P., 1997. Allometric regression equations to determine aerial biomasses of Mediterranean shrubs. Plant Ecol. 132, 59–69. https://doi.org/10.1023/A:1009765825024.

West, P.W., West, P.W., 2009. Tree and Forest Measurement,. vol. 20.. Springer. https://doi.org/10.1007/978-3-319-14708-6.

Wirth, C., Schumacher, J., Schulze, E.-D., 2004. Generic biomass functions for Norway spruce in Central Europe—a meta-analysis approach toward prediction and uncertainty estimation. Tree Physiol. 24, 121–139. https://doi.org/10.1093/treephys/24.2.121.

Xiang, W., Li, L., Ouyang, S., Xiao, W., Zeng, L., Chen, L., Lei, P., Deng, X., Zeng, Y., Fang, J., 2021. Effects of stand age on tree biomass partitioning and allometric equations in Chinese fir (*Cunninghamia lanceolata*) plantations. Eur. J. For. Res. 140, 317–332. https://doi.org/10.1007/s10342-020-01333-0.

Yang, H., Wang, Z., Tan, H., Gao, Y., 2017. Allometric models for estimating shrub biomass in desert grassland in northern China. Arid Land Res. Manag. 31, 283–300. https://doi.org/10.1080/15324982.2017.1301595.

Yang, X., He, P., Yu, Y., Fan, W., 2022. Stand canopy closure estimation in planted forests using a geometric-optical model based on remote sensing. Remote Sens 14, 1983. https://doi.org/10.3390/rs14091983.

Yao, X., Yang, G., Wu, B., Jiang, L., Wang, F., 2021. Biomass estimation models for six shrub species in Hunshandake sandy land in Inner Mongolia, Northern China. Forests 12, 167. https://doi.org/10.3390/f12020167.

Zambon, I., Colosimo, F., Monarca, D., Cecchini, M., Gallucci, F., Proto, A.R., Lord, R., Colantoni, A., 2016. An innovative agro-forestry supply chain for residual biomass: physicochemical characterisation of biochar from olive and hazelnut pellets. Energies 9, 526. https://doi.org/10.3390/en9070526.

Zewdie, M., Olsson, M., Verwijst, T., 2009. Above-ground biomass production and allometric relations of *Eucalyptus globulus* Labill. coppice plantations along a chronosequence in the central highlands of Ethiopia. Biomass Bioenergy 33, 421–428. https://doi.org/10.1016/j.biombioe.2008.08.007.

Zhao, Y., Liu, X., Wang, Y., Zheng, Z., Zheng, S., Zhao, D., Bai, Y., 2021. UAV-based individual shrub aboveground biomass estimation calibrated against terrestrial LiDAR in a shrub-encroached grassland. Int. J. Appl. Earth Obs. Geoinf. 101, 102358. https://doi.org/10.1016/j.jag.2021.102358.